JOURNAL OF MATERIALS SCIENCE 25 (1990) 1331–1334

The nitridation of austenitic Fe–29.8 Mn–7.4 Al–0.92 C and mainly ferritic Fe–32.3 Mn–8.8 Al–0.04 C alloys

J. J. CHAN, S. C. CHANG
Department of Materials Science and Engineering, National Tsing Hua University, Hsinchu, Taiwan

The nitridation of the austenitic Fe–29.8% Mn–7.4% Al–0.92% C and mainly ferritic Fe–32.3% Mn–8.8% Al–0.04% C alloys was studied. Plate-shaped AlN was observed in both alloys after heating in air and nitrogen at 1000° C. The scale formed on Fe–Mn–Al alloy with prolonged heating in air at 1000° C consists of several layers, from the innermost layer are first, AlN with Al-depleted austenite matrix; second, AlN with manganese-depleted ferrite matrix; and third, intermixed oxide which was only observed on alloys heated in air. Mechanisms of the formation of AlN scale were discussed.

1. Introduction

Based on economic and strategic considerations, research on the Fe–Mn–Al alloy system has attracted a lot of attention [1–3]. With a significant lowering in cost and in density, good mechanical properties [4], promising corrosion resistance [5] and oxidation resistance [6], alloys in the Fe–Mn–Al system are good candidates for replacing at least some Ni–Cr stainless steels.

For Fe–Mn–Al alloys, the austenitic structure is superior to the ferritic structure in the resistance of general corrosion [7, 8], hot corrosion [9], and stress corrosion cracking in NaCl solution [10]. For the oxidation of Fe–Mn–Al in pure oxygen, however, the fully ferritic structure is beneficial to the formation of a protective Al_2O_3 layer [11]. In contrast, the austenitic structure has a poor oxidation resistance [11, 12] on which no continuous Al_2O_3 was found.

When Fe–Mn–Al alloys were oxidized in dry air, a plate-shaped structure rich in aluminium was observed to form beneath the oxide scale. This structure has been identified as hexagonal AlN of the wustite (B4) type [13–15]. The formation of AlN could induce both the depletion and an uneven distribution of aluminium in the matrix, which resulted in the poor oxidation resistance of austenitic Fe–Mn–Al alloys.

Since the hot working of Fe–Mn–Al alloys is generally done at a temperature of about 1000° C, it is important to investigate the scale structure formed on Fe–Mn–Al alloys at 1000° C. In this work, the formation of AlN in Fe–Mn–Al alloys and its role on the oxidation resistance of the alloy in 1000° C air and nitrogen is reported.

2. Experimental procedure

Two Fe–Mn–Al alloys with the compositions given in Table I were prepared with an induction furnace under an argon-protective atmosphere. The ingots were homogenized at 1200° C for 4 h then hot rolled to 12.5 mm. After hot rolling, a 1 mm surface layer was removed by machining before cold rolling to 5.5 mm, annealing at 1000° C and oil quenching. The surface layer was ground off on SiC abrasive paper and specimens of the size 2 × 5 × 15 mm were cut from the material. The microstructure of alloy A was 90% ferrite and 10% austenite, while that of alloy B was fully austenitic.

Oxidation and nitridation were carried out in 1 atm air and commercially pure nitrogen at 1000° C up to 24 h. The morphology and microstructure of the tested specimen were studied by optical microscope and scanning electron microscope (SEM). The qualitative analysis was performed with an EDAX PV 9200/70 energy dispersive spectrometer. An X-ray diffractometer was used to identify the phases and the lattice parameters. A solution containing 6% perchloric acid and 94% acetic acid was used to dissolve the alloy matrix for observation of the scale structure.

3. Results

When alloy A was heated in nitrogen, plate-shaped AlN was formed beneath a manganese-rich transient scale layer. The growth of AlN into the alloy was quite uniform. After heating for 1.5 h the thickness of the AlN-containing region was about 75 μm. Figure 1 shows the polished cross section with the AlN region formed after 24 h heating in nitrogen. Figure 2 shows the white residue of AlN after matrix dissolution.

TABLE I Chemical composition of alloys

Alloy	Chemical composition (wt %)				Phases
	Mn	Al	C	Fe	
A	32.3	8.8	0.04	bal.	α + 10%γ
B	29.8	7.4	0.92	bal.	γ

0022–2461/90 $03.00 + .12

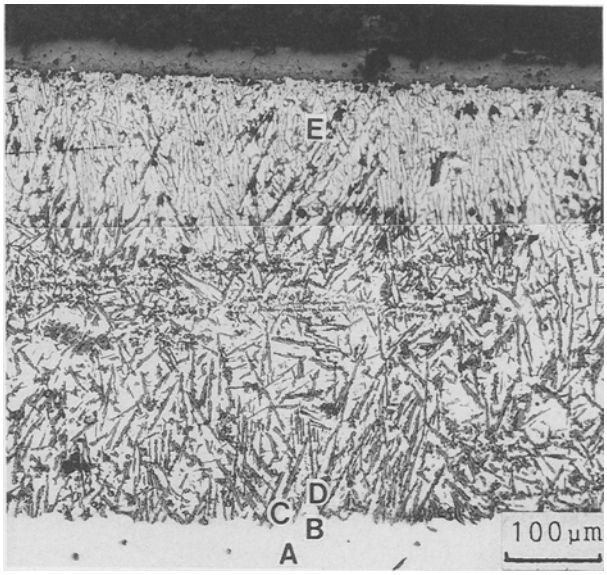

Figure 1 Polished cross section showing the AlN-containing region in alloy A heated in nitrogen for 24 h. For points A to E, see Fig. 3.

Figure 3 shows the EDAX results of the matrix at points shown in Fig. 1. In the AlN-containing layer, more than 30 μm behind the AlN front (D and E in Fig. 1), aluminium is almost totally depleted in the matrix. At point E in Fig. 1, which is close (40 μm) to the surface manganese-rich oxide layer, the manganese content is evidently lower than that of the bulk alloy. Similar results were observed in alloy A heated in air, and in alloy B heated in nitrogen.

X-ray diffraction shows that for both alloy A and alloy B heated in nitrogen, the phases in the AlN-containing layer just beneath the manganese-rich surface layer are AlN, ferrite and possibly spinel. The phases in the inner part of the AlN-containing layer are AlN, austenite and β-manganese. The measured lattice parameters of AlN were a = 0.311 and c = 0.498 nm, in agreement with previous reports [16–18]. The lattice parameters of the austenitic phase in alloys A and B were 0.366 and 0.368 nm, respectively. In the inner part of the AlN-containing region, where aluminium was depleted in the matrix, the lattice parameters were lowered to the ranges of 0.361 to 0.362, and 0.364 to 0.365 nm for alloys A and B, respectively.

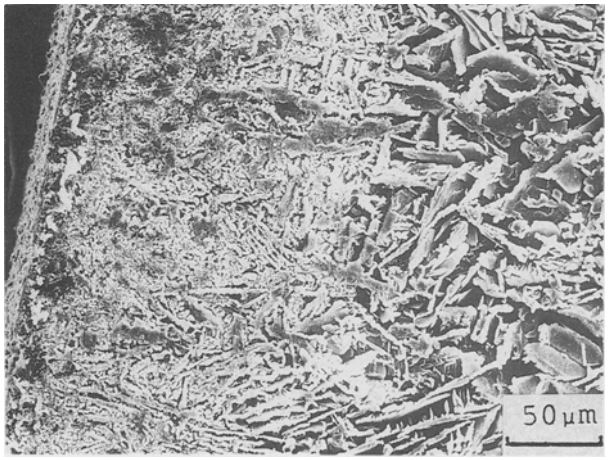

Figure 2 The observation of plate-shaped AlN after matrix dissolution.

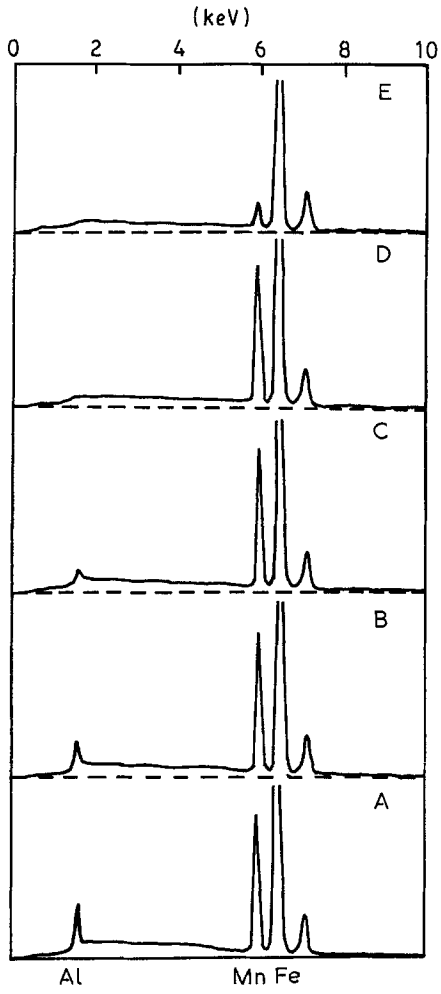

Figure 3 EDAX results of the matrix at points marked in Fig. 1: in the unreacted matrix (A), near the AlN front (B), 10 μm (C) and 30 μm (D) behind the AlN front, and 40 μm beneath the surface oxide layer (E).

When alloy A was heated in air at 1000° C for about 2 h, an adherent aluminium-rich oxide surface layer was observed with some AlN-containing nodules formed beneath it. As shown in Fig. 4, the front of the AlN nodules tended to become flat at a penetration depth of about 100 μm. After prolonged heating in air, the surface layer was made up of intermixed oxide in which the aluminium-rich spinel was embedded in oxide as shown in Fig. 5.

The typical microstructure of the scale formed on alloy A after heating in 1000° C air for 24 h, comprised three zones (Fig. 6). The outermost layer, as described above, consisted of intermixed oxide in which (Mn, Fe) Al_2O_4 and Al_2O_3 were embedded in the oxide of iron and manganese. Beneath the intermixed oxide, ferrite and AlN plate were the major phases. In the inner zone which lay between the ferrite zone and the unreacted matrix, the major phases were AlN and austenite.

After etching with 4% Nital (Fig. 7) a thin envelope of austenite could be observed in the front of the AlN-containing layer where the aluminium content was lowered by the formation of AlN. This kind of austenite envelope was also observed when this alloy is heated in nitrogen.

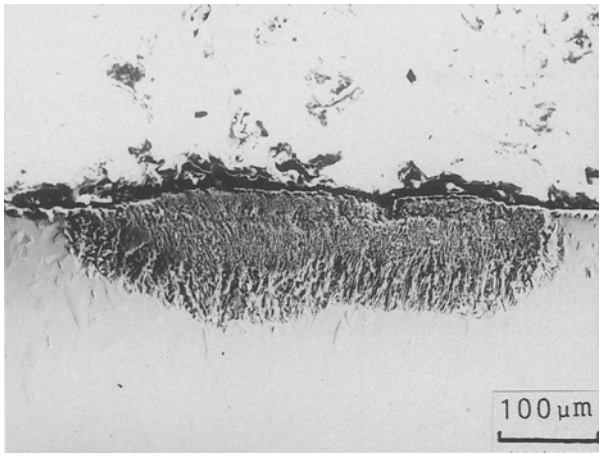

Figure 4 AlN nodule beneath the surface oxide was observed in alloy A heated in air for 2 h. The AlN front tended to become flat at a penetration depth of about 100 μm.

4. Discussion

Jackson and Wallwork [11] found that the alloys with compositions in the range of Fe–(5 to 10)% Mn–(6 to 10)% Al were fully ferritic and could form continuous adherent protective alumina scales in 600, 800 and 1000° C oxygen. For ferrite with a higher manganese content, nodule formation is observed to relate to the reaction of oxygen with manganese vapour at defects in the alumina scales. For the austenitic Fe–Mn–Al alloys, the aluminium content was less than 8% and was insufficient for the formation of protective alumina scale. Therefore they concluded that the austenite formed in ferritic alloys could be the site of breakdown of pre-existing alumina scales and of the subsequent growth of bulky manganese-rich oxides.

As shown in Fig. 4, the formation of AlN nodules was observed when alloy A was heated in air for 2 h. The nodules formed at scattered points while most of the surface area was covered by protective aluminium-rich scale. It is suggested that AlN nodules formed at weak points, such as austenite phase or flaws, in the initially protective aluminium-rich scale where nitrogen in the air could react with the substrate alloy. The nucleation and growth of AlN further decreases the aluminium content in the surrounding substrate, which prevents the healing of alumina film.

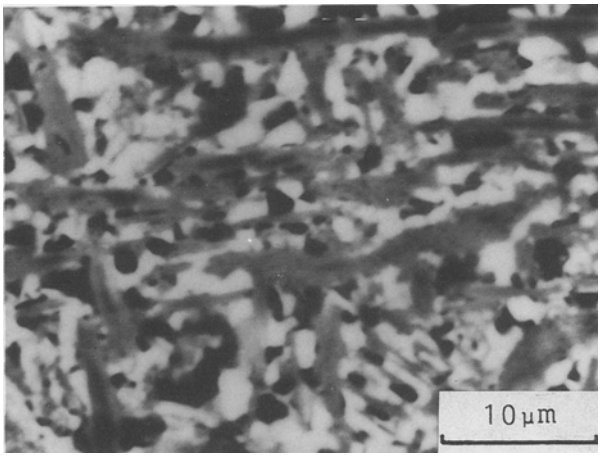

Figure 5 Intermixed oxide observed by SEM with composition contrast.

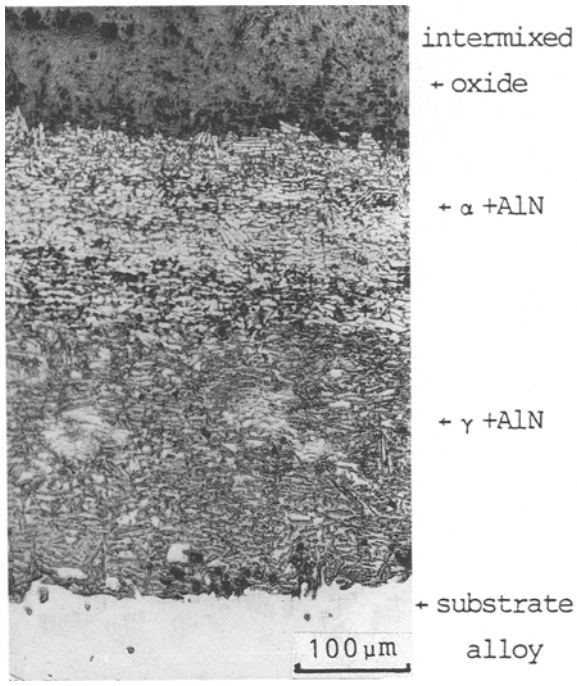

Figure 6 Typical microstructure of the scale on alloy A heated in air for 24 h.

In the later stage of heating, the unprotected matrix was oxidized and a displacement reaction

$$Mn + 2O_2 + 2AlN = MnO \cdot Al_2O_3 + N_2$$

could convert AlN to an oxide. This process leads to the formation of discontinuous Al_2O_3, (Fe, Mn) Al_2O_4, and intermixed oxide as shown in Fig. 5. The nitrogen released by the displacement reaction could diffuse further inward to the alloy to form new AlN there.

For Fe–Mn–Al alloys, manganese and carbon stabilize the austenitic structure, while aluminium stabilizes the ferritic structure. The formation of AlN results in the depletion and uneven distribution of aluminium in the matrix, which induces the transformation of ferrite into austenite to form the inner AlN and austenite zone. In the outer (near surface) part of the austenite zone, due to the high vapour pressure of manganese at 1000° C, the loss of manganese makes the ferrite phase more stable than the austenite phase again, and a ferrite layer beneath the intermixed oxide forms, as shown in Fig. 6.

In alloys A and B heated in nitrogen, ferrite and austenite zones were also observed in the outer and inner parts of the AlN-containing region, respectively. However in this case no intermixed oxide layer was observed.

When alloy A was heated in nitrogen or air, the reduction in aluminium content in the matrix around AlN plates makes the ferrite phase unstable. The thin austenite envelope in front of AlN in alloy A (Fig. 7) is a result of the lower aluminium content there. For the ferritic Fe–Al alloys heated at 500 and 575° C, the nucleation and growth of more-or-less equiaxial AlN particles has been reported [19]. In the austenitic Fe–31.3% Mn–7.6% Al–0.82% C alloy [15], the authors found that AlN grows along the (1 1 1) plane of the austenite matrix to form a plate shape. The

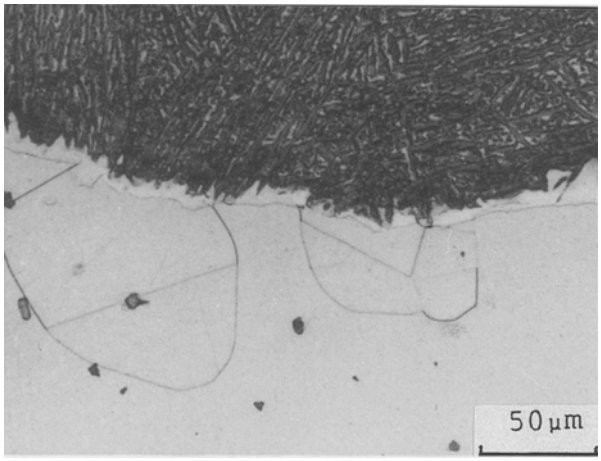

Figure 7 A thin envelope of austenite in front of AlN was observed after etching in alloy A heated in air.

orientation relationship between AlN and the fcc matrix was found to be

$$(0\,0\,0\,1)_{AlN} \parallel (1\,\bar{1}\,1)_{\gamma}$$

$$(2\,\bar{1}\,\bar{1}\,0)_{AlN} \parallel (1\,1\,0)_{\gamma}$$

$$[1\,0\,\bar{1}\,0]_{AlN} \parallel [\bar{1}\,1\,2]_{\gamma}$$

In this study, as shown in Fig. 2, plate-shaped AlN is observed not only in austenitic alloy B, but also in mainly ferritic alloy A. This implies that in this mainly ferritic alloy the AlN grew in a local environment similar to the austenitic alloy. It is proposed that once AlN nuclei formed, the low aluminium content could induce the transformation of ferrite around the nuclei into austenite to form an austenite envelope, as observed in the AlN front (Fig. 7). Then the AlN could grow behind the austenite envelope into plates, as observed here.

5. Conclusions

When mainly ferritic Fe–Mn–Al alloy A was heated in air at 1000° C for about 2 h, AlN nodules were observed to form under an initially protective aluminium-rich oxide. The front of the AlN nodules tends to become flat at a penetration depth of about 100 μm.

The scale formed on the Fe–Mn–Al alloy under prolonged heating in air at 1000° C consists of several layers. From the innermost layer are first, AlN with an aluminium-depleted austenite matrix due to the formation of AlN; second, AlN with a manganese-depleted ferrite matrix caused by the evaporation of manganese at high temperature; and third, an intermixed oxide layer formed by the replacement reaction.

When heated in nitrogen at 1000° C, the scale formed on Fe–Mn–Al alloys is similar to that formed in air except that a manganese-rich transient layer, but not an intermixed oxide layer, was observed.

Plate-shaped AlN was observed in both Fe–Mn–Al alloys A and B. The depletion of aluminium content in mainly ferritic Fe–Mn–Al alloy A due to the nucleation of AlN could induce the transformation of ferrite around the nuclei into austenite. Then the AlN in alloy A is able to grow behind the austenite envelope to form a plate shape, as in austenitic alloy B.

Acknowledgement

The authors are grateful for the support of the National Science Council, ROC, under grant NSC-77-0201-E007-06R.

References

1. J. S. DUNNING, M. L. GLENN and H. W. LEAVENWORTH JR, *Met. Prog.* **126** (1984) 19.
2. G. R. SMOLIK and S. K. BANERJI (eds) "Alternate Alloying for Environmental Resistance" (Metallurgical Society, Warrendale, 1987).
3. S. K. BANERJI, in Proceedings of the Workshop on Conservation and Substitution Technology Critical Materials, Nashville, Tennessee, June 1981.
4. S. K. BANERJI, *Met. Prog.* **113** (1978) 59.
5. R. WANG and F. H. BECK, *ibid.* **123** (1983) 72.
6. R. WANG, M. J. STRASZHEIM and R. A. RAPP, *Oxid. Met.* **21** (1984) 71.
7. A. P. BENTLEY, J. W. FOURIE and C. J. ALTSTETTER, in "Alternate Alloying for Environmental Resistance" (Metallurgical Society, Warrendale, 1987) p. 377.
8. S. C. CHANG, P. C. CHUNG and C. Y. SHIH, in "Corrosion/88" (NACE Research Symposium Paper) p. 19.
9. M. T. JAHN *et al.* in "Alternate Alloying for Environmental Resistance" (Metallurgical Society, Warrendale, 1987) p. 179.
10. S. C. CHANG, T. S. SHEU and C. M. WAN, in Proceedings of the 7th International Conference on the Strength of Metals and Alloys, August 1985, edited by H. J. Mcqueen *et al.* (Pergamon, Oxford) p. 1081.
11. P. R. S. JACKSON and G. R. WALLWORK, *Oxid. Met.* **21** (1984) 135.
12. C. H. KAO, C. M. WAN and M. T. JAHN, in "Alternate Alloying for Environmental Resistance" (Metallurgical Society, Warrendale, 1987) p. 347.
13. M. F. SILVA LOPES and F. C. RISSO ASSUNCAO, *ibid.* p. 321.
14. C. J. WANG and J. G. DUH, *J. Mater. Sci.* **23** (1988) 769.
15. J. J. CHAN and S. C. CHANG, *J. Mater. Sci. Lett.* **7** (1988) 787.
16. H. OTT, *Z. Physik* **22** (1924) 201.
17. G. A. JEFFREY, G. S. PARRY and R. L. MOZZI, *J. Chem. Phys.* **25** (1956) 1024.
18. K. M. TAYLOR and C. LENIE, *J. Electrochem. Soc.* **107** (1960) 308.
19. H. H. PODGURSKI and H. E. KNECHTEL, *Trans. TMS-AIME* **245** (1969) 1595.

Received 21 November 1988
and accepted 26 April 1989